This full text paper was peer reviewed at the direction of IEEE Communications Society subject matter experts for publication in the WCNC 2009 proceedings.

# Use of a Simplified Maximum Likelihood Function in a WLAN-Based Location Estimation

Shinsuke Hara and Daisuke Anzai
Graduate School of Engineering, Osaka City University
3-3-138, Sugimoto, Sumiyoshi-ku, Osaka 558-8585, Japan
Email: {hara@, daisuke@comm.}info.eng.osaka-cu.ac.jp

***Abstract*—In a location estimation with the received signal strength indication (RSSI) of a wireless signal in an area, the maximum likelihood (ML) function should match the real statistical property of the RSSI in the area. For a wireless local area network (WLAN)-based RSSI location estimation with a wideband signal in an office environment, the wideband signal experiences frequency selectively Rayleigh fading, so a complicated ML function containing several channel parameters needs to be derived in the environment. This paper shows that a simplified ML function containing only two channel parameters, which is optimum for a narrowband signal, is also applicable to an IEEE 802.11g WLAN-based location estimation with a wideband signal. Computer simulation and experimental results show that the use of the simplified ML function introduces almost no degradation in the location estimation performance in typical office environments, as compared with the use of an exact ML function.**

## I. Introduction

Location-based service is one of important context-aware services offered by wireless systems. Recently, wireless local area networks (WLANs) have become ubiquitous, so the location-based service with WLANs is attractive and advantageous. Current WLAN standards, such as the IEEE 802.11a, b and g, have the function of measuring received signal strength indication (RSSI) in their physical (PHY)/medium access control (MAC) layer protocols, so the RSSI has been often used in the WLAN-based location estimation.

RSSI-based location estimation methods are categeorized into two groups, such as statistical approach and deterministic approach. The former uses the statistical model between the RSSI and the distance between an access point and a target node whereas the latter called "fingerprinting" prepares the RSSI map (database) [1]. Even with a sophisticated algorithm such as maximum likelihood (ML) estimation, the statistical approach performs poorer, because in indoor environments, in addition to near/far effect, multipath fading as well as shadowing gives large variations to measured RSSIs.

To improve the performance of a WLAN-based ML location estimation, an ML function, which matches the real statistical property of the RSSI in the area where we intend to localize a target node, is required. However, the wideband signal in WLAN experiences frequency selective Rayleigh fading in the area, so the ML function has a complicated form containing several channel parameters, and furthermore, the number of channel parameters to be estimated makes the location estimation problem much more difficult.

This paper proposes the use of a simplified ML function, which is optimum for a narrowband signal, for WLAN-based location estimation with wideband signals.

This paper is organized as follows. Section II shows the system model and Section III outlines the maximum likelihood location estimation. Section IV explains the relationship between the multipath delay profile and the RSSI distribution for the signals with different bandwidths and Section V proposes the simplified ML function. Section VI demonstrates some computer simulation and experimental results. Finally, Section VII concludes the paper.

## II. System Model

In a location estimation area with size of $X_0$(width)$\times Y_0$ (depth)$\times Z_0$ (height), there are a stationary target node whose location is unknown and $J$ access points whose locations are known in advance. The locations of the target node and the $j$th access point ($j = 1, \cdots, J$) are respectively defined in vector forms as

$$\mathbf{t} = [x, y, h_t] \quad (1)$$

$$\mathbf{a}_j = [x_j, y_j, h_a] \quad (2)$$

where $x$ and $y$ are the unknown coordinates of the target node location, respectively, $x_j$ and $y_j$ are the known coordinates of the $j$th access point location, respectively, and $h_t$ and $h_a$ are the known heights of the target node and access point, respectively. With (1) and (2), the distance between the target node and the $j$th access point is calculated as

$$r_j = |\mathbf{t} - \mathbf{a}_j|. \quad (3)$$

The target node transmits $M$ "hello" packets to the access points and each access point measures an RSSI for every received packet. A computer gathers the information on the measured RSSIs through a sink node and finally estimates the location of the target node according to a location estimation algorithm in a centralized manner. The parameter vector composed of the unknown coordinates of the target node and the RSSI vector for the $j$th access point are defined as $\mathbf{q} = [x, y]$ and $\mathbf{P}_j = [P_j^1, \cdots, P_j^M]$, respectively, where $P_j^m$ denotes the RSSI of the $m$th packet transmitted from the target node and then measured at the $j$th access point.

978-1-4244-2948-6/09/$25.00 ©2009 IEEE

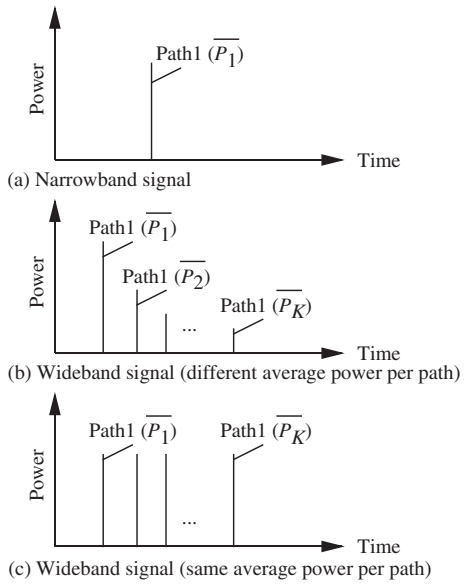


Fig. 1. Multipath delay profile: narrowband signal (a), and broadband signal (b) and (c).

## III. Maximum Likelihood Location Estimation

Assume that, for the location estimation area, the probability density function (*pdf*) of the RSSI vectors $\mathbf{P}_1, \cdots, \mathbf{P}_J$ given $\mathbf{q}$ and $\mathbf{c}$ ($\mathbf{c}$ is an unknown parameter vector) has been obtained as $p(\mathbf{P}_1, \cdots, \mathbf{P}_J|\mathbf{q}, \mathbf{c})$. In this case, the log-likelihood function on $\mathbf{q}$ and $\mathbf{c}$ is defined as

$$L(\mathbf{q}, \mathbf{c}) = \log p(\mathbf{P}_1, \cdots, \mathbf{P}_J|\mathbf{q}, \mathbf{c}). \tag{4}$$

Assuming that $P_j^m$ is independent of $P_j^{m'}$ ($m \neq m'$) (*temporal whiteness*) (see Appendix A) and $P_{j'}^m$ ($j \neq j'$) (*geographical whiteness*), (4) is rewritten as

$$L(\mathbf{q}, \mathbf{c}) = \sum_{j=1}^{J} \sum_{m=1}^{M} \log p(P_j^m|\mathbf{q}, \mathbf{c}) \tag{5}$$

where $p(P_j^m|\mathbf{q}, \mathbf{c})$ denotes the *pdf* of $P_j^m$ given $\mathbf{q}$ and $\mathbf{c}$. Furthermore, having known the parameter vector by a pre-measurement, the maximum likelihood (ML) estimation gives $\hat{\mathbf{q}}$ which maximizes (5):

$$\frac{\partial L(\mathbf{q}, \mathbf{c})}{\partial \mathbf{q}} = 0. \tag{6}$$

## IV. Selection of $p(P_j^m|\mathbf{q}, \mathbf{c})$

The *pdf* of the RSSI $p(P_j^m|\mathbf{q}, \mathbf{c})$ is unknown in reality so we need to select its appropriate form with the parameter vector $\mathbf{c}$. Fig.1 (a) shows the multipath delay profile of a channel for a narrowband signal. As compared with the coherence bandwidth of the channel, the signal bandwidth is narrow enough, so there is a single path in the profile resulting in frequency non-selective Rayleigh fading. For instance, this profile is applicable to the IEEE 802.15.4 signal with bandwidth of 2MHz developed for wireless personal area networks (WPANs) [2], and in this case, the variation of the RSSI can be well modeled with the following two-layered model: [3],[4] (the superscript $m$ is dropped with no loss of generality)

$$p_n(P_j|\mathbf{q}, \mathbf{c}_n) = \frac{1}{\overline{P}_j(\mathbf{q}, \mathbf{c}_n)} \exp\left(-\frac{P_j}{\overline{P}_j(\mathbf{q}, \mathbf{c}_n)}\right) \tag{7}$$

$$\overline{P}_j(\mathbf{q}, \mathbf{c}_n) = \alpha r_j^{-\beta} \tag{8}$$

$$\mathbf{c}_n = [\alpha, \beta]^T \tag{9}$$

where $\overline{P}_j$ denotes the average signal power received at the $j$th access point, and $\alpha$ and $\beta$ are the two channel parameters such as attenuation factor and power decay factor, respectively, which are uniquely determined by the location estimation area.

On the other hand, as the signal bandwidth increases, the number of resolvable paths increases in a multipath delay profile. Fig.1 (b) shows the multipath delay profile of a channel for a wideband signal. In the profile, there are $K$ paths resulting in frequency selective fading. Here, the arrival time of each path gives no effect to the received power distribution, so it has been dropped. This profile may be applicable to the IEEE 802.11g signal with bandwidth of 20MHz [5], so when the average power of each path is different, the variation of the RSSI is modeled with the following two-layered model: (see Appendix B)

$$p_{wd}(P_j|\mathbf{q}, \mathbf{c}_{wd}) = \frac{1}{\prod_{k=1}^{K} \overline{P}_{jk}} \cdot \sum_{k=1}^{K} \frac{\exp\left(-\frac{P_j}{\overline{P}_{jk}}\right)}{\prod_{\substack{l=1 \\ l\neq k}}^{K} \left(1/\overline{P}_{jl} - 1/\overline{P}_{jk}\right)} \tag{10}$$

$$\overline{P}_j(\mathbf{q}, \mathbf{c}_{wd}) = \sum_{k=1}^{K} \overline{P}_{jk} \tag{11}$$

$$\overline{P}_j(\mathbf{q}, \mathbf{c}_{wd}) = \alpha r_j^{-\beta} \tag{12}$$

$$\mathbf{c}_{wd} = [\alpha, \beta, K, \overline{P}_1, \cdots, \overline{P}_{K-1}]^T \tag{13}$$

where $\overline{P}_{jk}$ is the average signal power through the $k$th path received at the $j$th access point. This channel model has $K+2$ channel parameters, so it is very difficult to determine their values from the data obtained in the pre-measurement. *Therefore, we assume that each path has the same average power* ($= \overline{P}_j(\mathbf{q}, \mathbf{c}_{wd})/K$) *in the profile.* Fig.1 (c) shows the uniform multipath delay profile, and in this case, with a chi-square distribution with $2K$ degrees of freedom, the variation of the RSSI is modeled as

$$p_{we}(P_j|\mathbf{q}, \mathbf{c}_{we}) = \frac{1}{(K-1)!} \left(\frac{1}{\overline{P}_j(\mathbf{q}, \mathbf{c}_{we})/K}\right)^K \cdot P_j^{K-1} \exp\left(-\frac{P_j}{\overline{P}_j(\mathbf{q}, \mathbf{c}_{we})/K}\right) \tag{14}$$

$$\overline{P}_j(\mathbf{q}, \mathbf{c}_{we}) = \alpha r_j^{-\beta} \tag{15}$$

$$\mathbf{c}_{we} = [\alpha, \beta, K]^T. \tag{16}$$

This model has only three channel parameters.

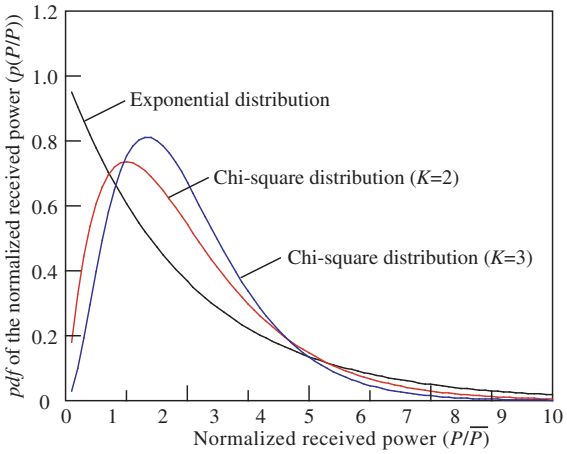


Fig. 2. Distribution of the received power with the uniform multipath delay profile.

Fig.2 shows the distribution of the received power (RSSI) normalized by the average for $K$ =1, 2 and 3. For the case of $K = 1$ corresponding to the narrowband signal case, the received power widely fluctuates, but as $K$ increases, in other words, as the signal bandwidth becomes wide, it tends to concentrate on the average. From this figure, we can intuitively understand that the signal with wider bandwidth brings better location estimation performance.

## V. Simplified ML Function

For the case of the narrowband signal, by substituting (7) and (8) into (6), we have the equation to solve for the ML location estimation. *Taking into consideration that $\overline{P}_j$ is only a function of* $\mathbf{q}$, we have

$$\frac{\partial L_n(\mathbf{q}, \mathbf{c}_n)}{\partial \mathbf{q}} = \frac{\partial}{\partial \mathbf{q}} \sum_{j=1}^{J} \sum_{m=1}^{M} \left( \log \frac{1}{\alpha r_j^{-\beta}} - \frac{P_{jm}}{\alpha r_j^{-\beta}} \right) = 0. \quad (17)$$

On the other hand, for the case of the wideband signal with the uniform multipath delay profile, by substituting (14) and (15) into (6), we have

$$\frac{\partial L_{we}(\mathbf{q}, \mathbf{c}_{we})}{\partial \mathbf{q}} = K \frac{\partial}{\partial \mathbf{q}} \sum_{j=1}^{J} \sum_{m=1}^{M} \left( \log \frac{1}{\alpha r_j^{-\beta}} - \frac{P_{jm}}{\alpha r_j^{-\beta}} \right) = 0. \quad (18)$$

We can see that (18) is $K$ times as large as (17) but it does not affect the solution. Namely, for a given set of $P_{11}, \cdots, P_{JM}$, (17) and (18) give the same solution on the location of the target node. This means that, *if the wideband signal has the uniform multipath delay profile in the location estimation area, the (simplified) ML function for the narrowband signal is applicable to the location estimation with the wideband signal, where we do not have to estimate the number of paths in the multipath delay profile any more.* This result is very interesting. From Fig.2, we can see that the statistical properties of the narrowband and wideband signals are totally different, so this means that we can accept a mismatch between the real statistical property of the RSSI in the area and the ML function used for location estimation. The reason is that the exponential and chi-square distribution functions are parameterized by only the average power (per path) (see (7) and (14)), so the location estimators try to calculate the average power thus the average distance between an access point to the target node. This mechanism can be seen in the last term of (17) and (18).

In reality, each path in the multipath delay profile has a *different* power (we call this "a realistic situation"), so if we apply the simplified ML function to the realistic situations, the location estimation performance degrades. In the following section, we will evaluation the performance degradation in realistic situations.

TABLE I
Parameters in the simplified TGn channel models.

| Model | A | B | C | D | E | F |
|---|---|---|---|---|---|---|
| Path1 [dB] | 0 | 0 | 0 | 0 | 0 | 0 |
| Path2 [dB] | | -1.8 | -5.1 | -10.5 | -1.5 | -0.4 |
| Path3 [dB] | | | | -23.4 | -9.1 | -6.1 |
| Path4 [dB] | | | | | -20.4 | -12.3 |
| Path5 [dB] | | | | | | -15.6 |
| Path6 [dB] | | | | | | -20.3 |

## VI. Evaluation of the Performance Degradation in Realistic Situations

We evaluate the performance degradation for the use of the simplified ML function in location estimation by a computer simulation and an experiment.

### A. Computer Simulation

In the computer simulation, we use the TGn channel models [6], which are originally developed to describe the spatio-temporal structures of the channel impulse responses often encountered in office environments. Here, we do not care about their spatial structures, so we simplify them to have only temporal structures, resulting in multipath delay profiles. Table I summarizes the average power of each path in the simplified TGn multipath delay profile models, where the power of each path is exponentially distributed.

Fig.3 shows the layout of a location estimation area in the computer simulation. In the area, there are five access points and a target node, and the heights of the access point and target node are set to $h_t = h_a$ =1.3m. Furthermore, the attenuation factor and the power decay factor are set to $\alpha = 1.43 \times 10^{-5}$ and $\beta = 1.84$.

Fig.4 shows the root mean square (RMS) location estimation error versus the number of transmitted packets ($M$) for 10,000 different locations of the target node. For each model, two curves are shown; the packets are generated according to the multipath delay profile in TABLE I and the corresponding exact ML function is used in location estimation for one case

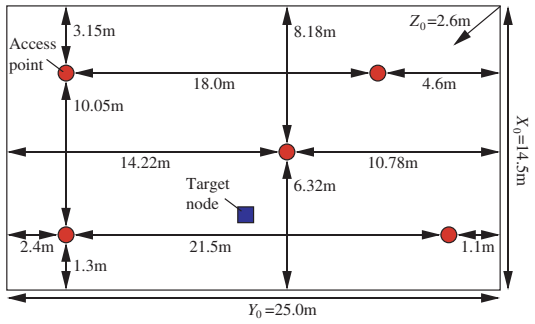


Fig. 3. Layout of the location estimation area in the computer simulation and the experiment.

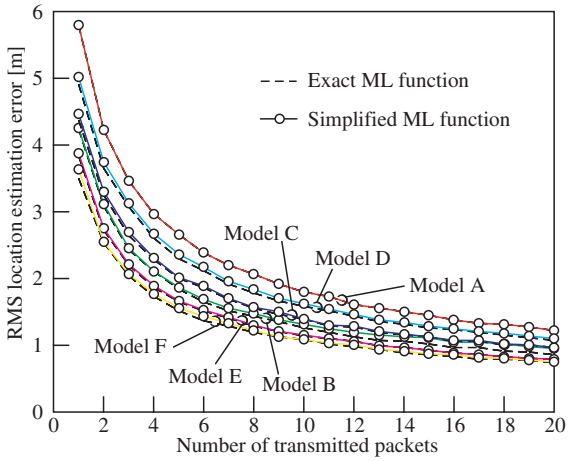


Fig. 4. Computer simulation result on the RMS location estimation error versus the number of transmitted packets ($M$).

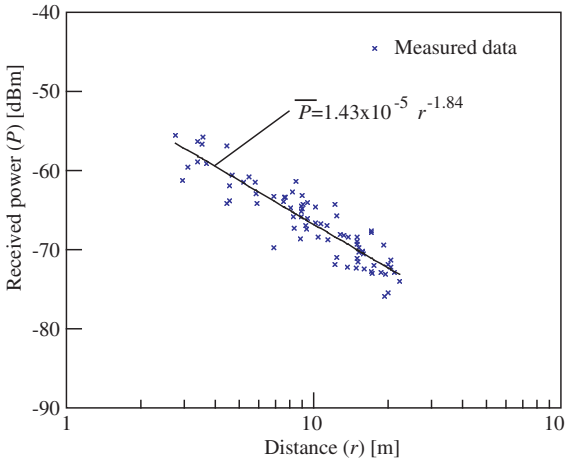


Fig. 5. RSSI versus the distance for Wi-Fi.

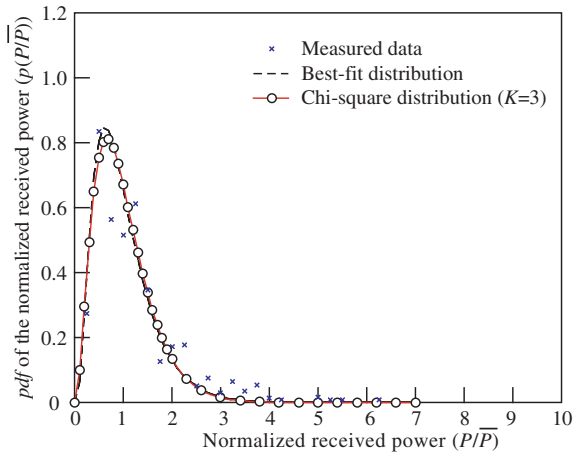


Fig. 6. *pdf* of the RSSI for Wi-Fi.

(broken line) whereas the simplified ML function is used for another case (solid line). Here, the model A has only one path in the multipath delay profile corresponding to the narrowband signal case, so there is no different between the exact and simplified ML functions. As shown in TABLE I, the models B-F have the different average power for each path, but the location estimation performance with the simplified ML function is almost the same as the one with the exact ML function. Therefore, in typical office environments, the use of the simplified ML function reduces the number of channel parameters so as to have only two channel parameters such as $\alpha$ and $\beta$, and show almost the same location estimation performance as the use of the exact ML function.

### *B. Experiment*

For a typical office room with the same layout as shown in Fig.3, we conducted an experiment on location estimation with five Wi-Fi access points and a target node based on the IEEE 802.11g standard (WLAN). In addition, for comparison purpose, we conducted the same experiment with Zigbee nodes based on the IEEE 802.15.4 standard (WPAN).

Figs.5 and 6 show the measured RSSI versus the distance and the *pdf* of the RSSI for the Wi-Fi WLAN, respectively. From Fig.5, we can see that $\alpha = 1.43 \times 10^{-5}$ and $\beta = 1.84$ is a good fit. In Fig.6, the best-fit distribution is given by (10) with $K = 4$ and the average path gains=0dB, -1dB, -6dB and -9dB (the fitting coefficient between the measured data and the theoretical curve is 0.954) whereas the chi-square distribution is given by (14) with $K = 3$ (the fitting coefficient between the measured data and the theoretical curve is 0.952).

On the other hand, Figs.7 and 8 show the measured RSSI versus the distance and the *pdf* of the RSSI for the Zigbee WPAN, respectively. From these figures, we can see that the *pdf* of the RSSI is exponentially distributed as (7) with $\alpha = 3.09 \times 10^{-5}$ and $\beta = 2.51$ in (8) (the fitting coefficient is 0.971).

Finally, Fig.9 shows the experimental result on the RMS location estimation error versus the number of transmitted packets ($M$) for 16 different locations of the target node. The performance with the Wi-Fi access points and target node is much better than the one with the Zigbee nodes; around 4.3m for the Zigbee nodes whereas around 2.3m for the Wi-Fi access points and target node. There is no large difference in the achievable RMS location estimation error between the two ML functions; 2.30m for the best-fit ML function whereas

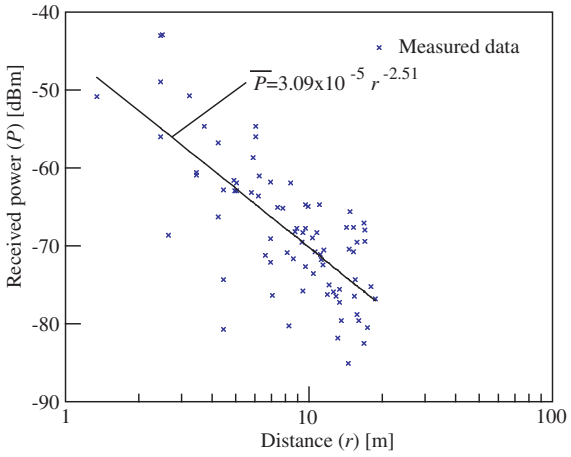


Fig. 7. RSSI versus the distance for Zigbee.

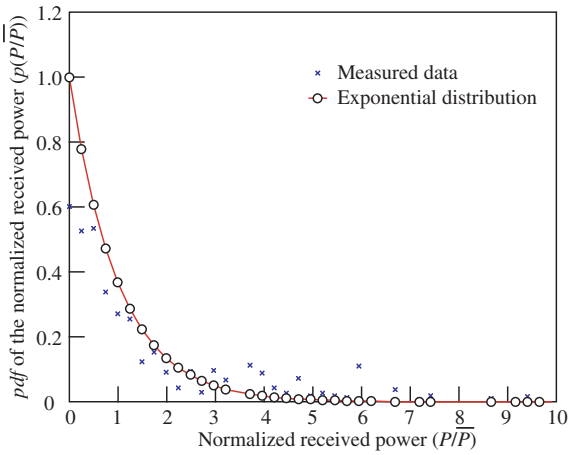


Fig. 8. *pdf* of the RSSI for Zigbee.

2.37m for the simplified ML function.

## VII. Conclusions

This paper has shown that a simplified ML function, which is optimum for a narrowband signal subject to frequency non-selective Rayleigh fading, is applicable to a WLAN-based location estimation with RSSI where the signal is subject to frequency selective Rayleigh fading. The computer simulation and experimental results have revealed that, in an IEEE 802.11g WLAN-based location estimation, as compared with the use of an exact ML function containing several channel parameters, the performance degradation associated with simplification of the ML function is negligibly small in typical office environments.

The simplified ML function contains only two channel parameters to be estimated, so a joint channel parameter/target node location estimation is easily applicable to WLAN-based location estimation [4], which totally avoids troublesome pre-measurement for estimating the channel parameters.

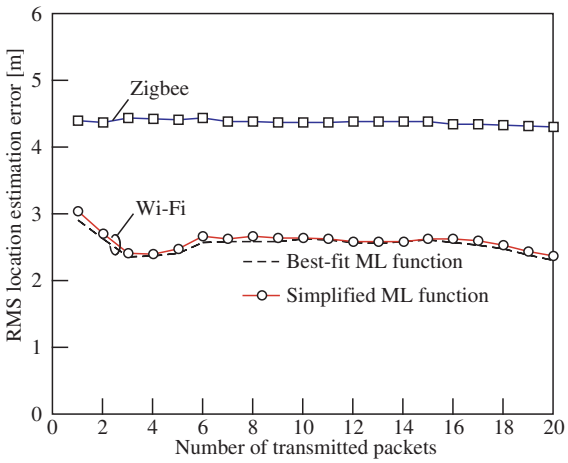


Fig. 9. Experimental result on the RMS location estimation error versus the number of transmitted packets ($M$).

## Appendix A: Temporal Autocorrelation Function in an Indoor Channel

The channel between a target node and an access point (an anchor node) can be modeled as a model where there are a stationary receiver with a monopole antenna, a stationary transmitter with a monopole antenna and $L$ moving reflectors (walking men). When the receiver antenna is horizontally polarized, it has a directivity on the horizontal plane, but it is assumed that the directivity can be ignored because the signals transmitted from the transmitter arrive at the receiver antenna with larger depression angles. Fig.10 shows the model, where it is furthermore assumed that each reflector is moving with speed of $v$ m/sec in a randomly chosen direction. The received signal can be written in the equivalent baseband expression as

$$z(t) = \sum_{l}^{L} g_l e^{2\pi f_D (cos\xi_l)t} \tag{19}$$

where $g_l$ and $\xi_l$ are the complex channel gain for the $l$th reflector and the angle between the direction from the receiver to the $l$th reflector and the moving direction of the $l$th reflector, respectively. The angle $\xi_l$ can be considered to be uniformly distributed in [0, $2\pi$], so (19) shows that the indoor channel under the above assumption can be modeled as the Jakes' model [7]. Therefore, the normalized autocorrelation function of the channel in terms of complex envelope is given by

$$\rho(\tau) = J_0(2\pi f_D \tau) \tag{20}$$

where $J_0(\cdot)$ and $f_D$ are the *zero*th order Bessel function of the first kind and the maximum Doppler frequency, respectively. Defining the wavelength of the carrier and the distance as $\lambda$ and $\delta$, respectively, with the following relationships:

$$f_D = v/\lambda \tag{21}$$

$$\delta = v\tau \tag{22}$$

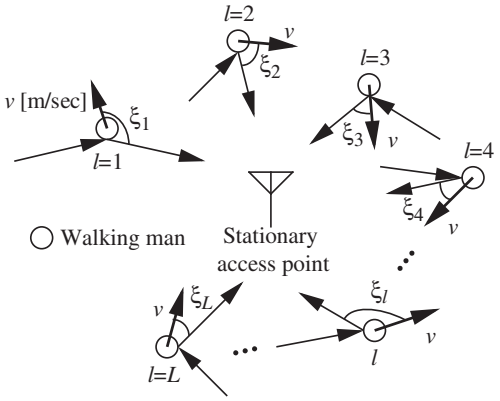


Fig. 10. An indoor channel model.

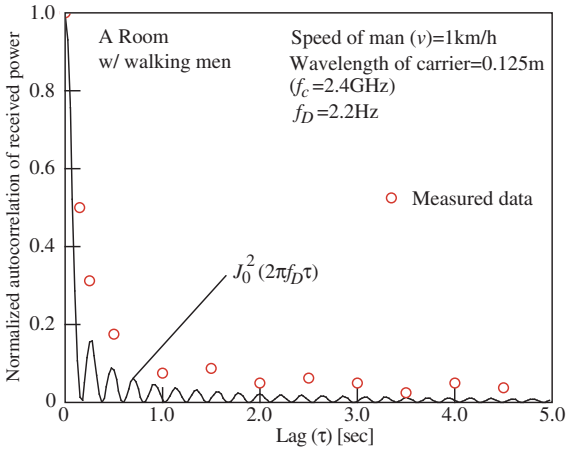


Fig. 11. Envelope correlation function.

the normalized fading correlation between two locations with distance of $\delta$ is written as

$$\rho(\delta) = J_0(2\pi\delta/\lambda). \tag{23}$$

Fig.11 compares the autocorrelation function of the channel in terms of power measured in a room with the one theoretically derived from Jakes' model for $v$=1.0km/h and $\lambda$=0.125m (carrier frequency=2.4GHz). Here, the autocorrelation function in term of power is given by [7]

$$\rho_{power}(\tau) = J_0^2(2\pi f_D \tau). \tag{24}$$

We can see from the figure that the experimental result agrees with the theoretical result. This fact shows that Jakes' model is applicable to the indoor environment and furthermore the assumption of "temporal whiteness" holds for WiFi and Zigbee (operating in the 2.4GHz band) discussed in this paper for the case of "hello" packet interval more than 0.2sec, because the temporal correlation between successive two packets becomes less than 0.3.

## Appendix B: Derivation of the Probability Function of the RSSI

The *pdf* of the RSSI for the *k*th path and the characteristic function defined as Laplace Transform of the *pdf* are respectively written as

$$p_n(P_{jk}|\mathbf{q}, \mathbf{c}_n) = \frac{1}{\overline{P}_{jk}} \exp\left(-\frac{P_{jk}}{\overline{P}_{jk}}\right) \tag{25}$$

$$\begin{aligned} \phi_k(s) &= L[p_n(P_{jk}|\mathbf{q}, \mathbf{c}_n)] \\ &= \int_0^{+\infty} p_n(P_{jk}|\mathbf{q}, \mathbf{c}_n) e^{-sP_{jk}} dP_{jk} \\ &= \frac{1/\overline{P}_{jk}}{s + 1/\overline{P}_{jk}}. \end{aligned} \tag{26}$$

The characteristic function of the sum of $P_{j1} \cdots P_{jK}$ ($P_j = P_{j1} + \cdots + P_{jK}$) is given by the product of their characteristic functions, so it is written as

$$\phi_w(s) = \prod_{k=1}^{K} \phi_k(s). \tag{27}$$

When $\overline{P}_{jk}$ is different, taking the inverse Laplace Transform of (27) leads to (10), whereas when $\overline{P}_{jk}$ is identical, it leads to (14).

## Acknowledgement

This study was supported in part by a Grant–in–Aid for Scientific Research (No. 19360177) from the Ministry of Education, Science, Sport and Culture of Japan.

## References

[1] P.Bahl and V.N.Padmanabhan, "RADAR: An In-building RF-Based User Location and Tracking System," *Proc. IEEE INFOCOM*, pp.775-784, Mar. 2000.
[2] Wireless Medium Access Control (MAC) and Physical Layer (PHY) Specifications for Low-Rate Wireless Personal Area Networks (WPANs), IEEE Std.802.15.4, 2003.
[3] S. Hara, D. Zhao, K. Yanagihara, J. Taketsugu, K. Fukui, S. Fukunaga and K. Kitayama, "Propagation Characteristics of IEEE 802.15.4 Radio Signal and Their Application for Location Estimation," *Proc. IEEE VTC 2005-Spring*, pp. 97-101, May 2005.
[4] Z. Radim, S. Hara, K. Yanagihara and K. Kitayama, "A Joint Estimation of Target Node Location and Channel Model Parameters in an IEEE 802.15.4 Based Sensor Network," *Proc. IEEE PIMRC2007*, in CD-ROM, Sept. 2007.
[5] Wireless LAN MAC and PHY Specifications Amendment 4: Futher Higher Rate Extension in the 2.4 GHz Band, IEEE Std.802.11g-2003 Part II.
[6] IEEE 11-03/940r5, TGn Channel models.
[7] W.C.Y.Lee, *Mobile Communications Engineering,* McGraw-Hill, 1982.